Photonik
Ingenieurbüro
Dr. Walter Luhs

LT-0200
Glass Fibre Optics

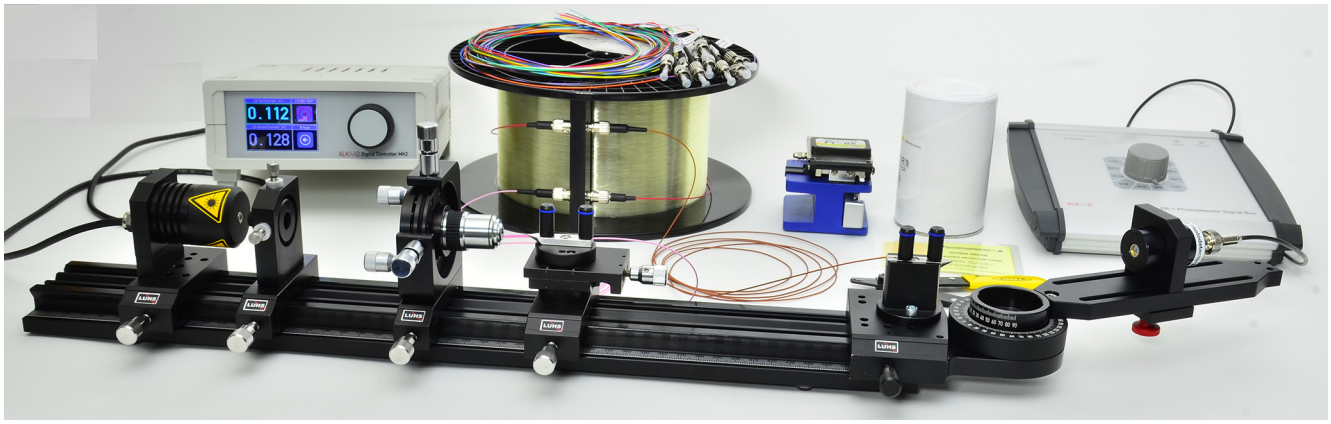

Table of Contents

1.0 INTRODUCTION **3**

2.0 BASICS **3**

2.1 Coupling of light to fibre *6*

2.2 Properties of laser diodes *8*

2.3 Ge and Si PIN-diodes *9*

3.0 EXPERIMENTS **11**

3.1 Experimental set-up *11*

3.2 Description of the components *11*

3.2.1 Digital Diode Laser Controller 14

3.2.2 Diode laser controller screens 14

4.0 PREPARATION OF THE FIBRE **16**

4.1 Properties of the laser diode *17*

4.2 Measurements with the fibre *18*

4.2.1 Measure the numerical aperture 19

4.2.2 Transit time measurement 19

5.0 LASER SAFETY REMARKS **20**

1.0 Introduction

The basic idea to use guided light for data communication was published in 1939 by H. Buchholz in his paper „Die Quasioptik der Ultrakurzwellenleiter“ (The quasi optical behaviour of ultra short wave guides). However it took more than 20 years to develop first realistic technical solutions mainly encouraged by the first available diode lasers in 1962. These new light sources are ideally suited as transmitter because of their ability to be modulated and in addition, as we know today, they can be produced in large numbers at low prices. Nowadays the world wide communication is based on fibre optics combined with laser diodes and the development in this area belongs to the most exciting ones in this century. In 1977 based on the experience and results rapid investigation in other fields than communications were initiated, leading for example in the development of fibre gyros for navigation purposes of air planes. In principle this new technology does not require a new understanding of the physics because the related phenomena are well known and can be considered as a combination of classical optics and lasers.

However for the realisation a lot of technical problems had to been solved. In the fibres mainly used in communication the light is guided within a „glass tunnel“ with a diameter of 9 µm only. The necessary mechanical components as well the production process of the fibres itself were subject of comprehensive developments. Considerable efforts today are undertaken to reduce fibre transmission losses by using so called active fibres and in the realisation of integrated optical devices for distributing and receiving signals. The field of fibre optics is still expanding and of high common interest. Therefore this experiment is considered as a introduction to this important technology.

The trainees are introduced firstly to prepare a bare optical fibre in such a way that suitable end faces are obtained. This process of fibre stripping and cleaving is a recurrent practice either in research labs or telecommunication.

By means of collimation optics the beam of the diode laser is made almost parallel before it enters the microscope objective which focuses the light into the multimode fibre. By observing the output at the exit of the fibre the coupling efficiency is optimised by adjusting the precise mounts. Once a strong signal has been obtained the numerical aperture of the fibre is measured by means of the photodetector mounted to the pivot arm.

In a next step the photodetector is connected to an oscilloscope and the injection current of the diode laser is modulated. Both the diode laser signal and fibre output are displayed on the scope and the time of flight becomes apparent and can be measured. From this measurement either the speed of light or the length of the fibre is determined.

2.0 Basics

There is hardly any book in optics which does not contain the experiment of Colladan (1861) on total reflection of light. Most of us may have enjoyed it during the basic physics course.

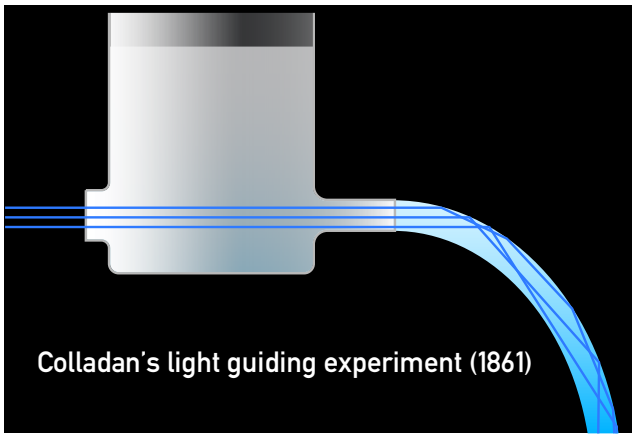

Fig. 1: Colladan's experiment for the demonstration of the total reflection of light (1861).

A light beam is guided into the outlet of a reservoir which is filled with water. When the outlet is opened, a considerable amount of light follows inside the water jet. It is expected that the jet would remain dark unless it contains small disturbances. This leads to a certain scatter of the light and the jet appears illuminated all along its way. Effects of light created in this way are also known as „fontaines lumineuses“. They generally please the spectators of water games.

This historical experiment of Colladan already shows the physical phenomena which are basic of fibre optics. The difference of Colladan's light conductor to modern fibres is the dimension which for a fibre is in the order of magnitude of the wavelength λ of light. Let the diameter of a light guide d_L, we can state:

„Fontaines lumineuses“	$d_L >> \lambda$
Multimode fibres	$d_L > \lambda$
Singlemode fibres	$d_L \approx \lambda$

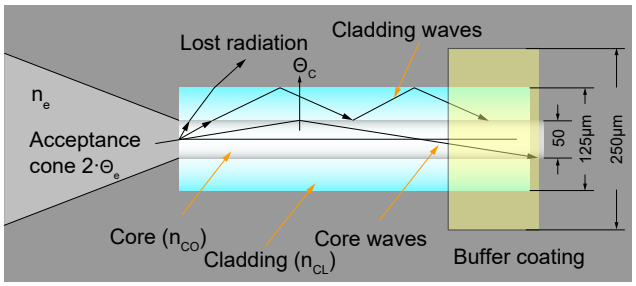

Fig. 2: Multimode step index fibre

The Fig. 2 shows the principle of a multimode fibre typically used for short range (< 4-5 km) applications. For telecommunication application the fibre consists of a core with a typical diameter of 50 µm or 62.5 µm (imperial dimension) which is surrounded by a cladding with a diameter of 125 µm (surprisingly for both the metric and imperial world). Finally a tight buffer coating consisting of an acrylic polymer protects the fibre against breaking and other environmental impacts. The diameter is typically 250 µm. The path of the light rays inside the fibre can be traced by using the laws of geometric optics. However, if the core diameter of the optical fibre is reduced to obtain a singlemode fibre, the simple geometric optics fails and requires the solution of the Maxwell equations including the boundary conditions of optical fibre.

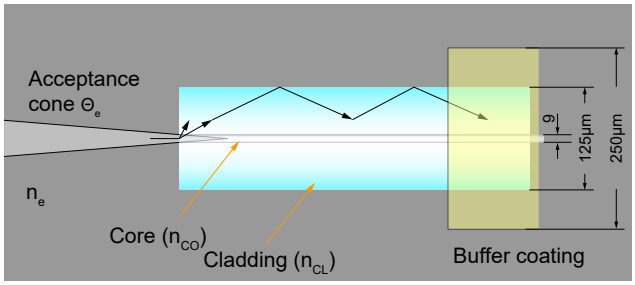

Fig. 3: Singlemode step index fibre

From Fig. 3 one can guess that a classical treatment will not deliver correct results.
However, Fig. 2 reveals some facts which can be obtained without having solved Maxwell's equations. Taking off from geometrical considerations we can state that there must be a limiting angle Θc for total reflection at the boundary between cladding and core.

$$\cos(\Theta_c) = \frac{n_{CL}}{n_{CO}} \qquad \text{eq. 1}$$

To obtain the angle of incidence we apply the law of refraction:

$$\frac{\sin(\Theta_e)}{\sin(\Theta_c)} = \frac{n_{CO}}{n_e}$$

and obtain:

$$\Theta_e = \arcsin\left(\frac{n_{CO}}{n_e} \cdot \sin\Theta_c\right)$$

Using eq. 1 along with $n_o \approx 1$ for air we finally get:

$$\Theta_e = \arcsin\left(\sqrt{n_{CO}^2 - n_{CL}^2}\right)$$

The limiting angle Θ_e represents the half opening angle of a cone. All beams entering within this cone will be guided inside the core by total reflection. As common in optics here, too, we can define a numerical aperture A:

$$A = \sin\Theta_e = \sqrt{n_{CO}^2 - n_{CL}^2} \qquad \text{eq. 2}$$

These are the results we can gain straight forward by applying the geometrical optics. It gives us already a base for understanding the light transport inside a multimode fibre. Already at this point we may detect a weakness of multimode fibres.

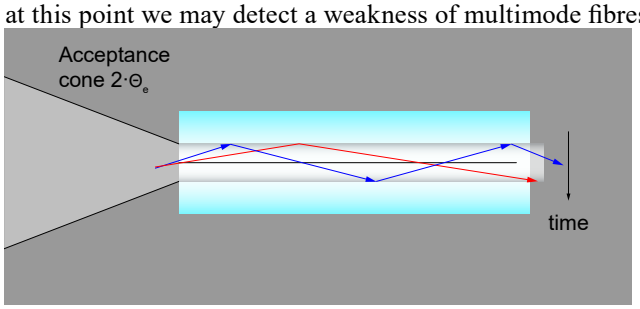

Fig. 4: Different covered distances inside the fibre core

The eq. 2 states that all light rays entering within the cone defined by the angle Θ_e will be guided by the fibre. However, due to their different angle of incidence some photons need a longer time than others. This effect limits the usable data rate of such a multimode fibre. Assuming an input pulse with sharp on and off transition will appear at the end of the fibre as a smeared out pulse. To avoid this bandwidth limiting effects, the number of internal reflections must be reduced. Best of all there should be no reflection at all. This lead to the development of the singlemode optical fibre.
For a deeper understanding of the mode generation and their properties Maxwell equations with respect to the fibre boundary conditions are needed to be solved. We will just show the road map of the solution and discuss the results out of it. Based on the general Maxwell equations we derive the fundamental wave equations for a wave propagating in a medium.

$$\Delta\vec{E} - \frac{n^2}{c^2} \cdot \frac{\partial^2 \vec{E}}{\partial t^2} = 0 \qquad \text{eq. 3}$$

$$\Delta\vec{H} - \frac{n^2}{c^2} \cdot \frac{\partial^2 \vec{H}}{\partial t^2} = 0 \qquad \text{eq. 4}$$

It makes sense to assign the coordinates in such a way that the propagation axis of the fibre is the z-direction. It may propagate in zigzag or any other way. Therefore we introduce the general coefficient for the propagation as β which will be determined in the course of subsequent calculations. Adapted to the geometry of the fibre we write the general electrical field as combination of a radial E_r, azimuthal E_φ and a field component propagating in z (E_z):

$$E_r(r,\varphi,z,t) = (\hat{E}_r \cdot e^{i\omega t} + \hat{E}_r^* \cdot e^{-i\omega t}) \cdot e^{-i\beta \cdot z}$$
$$E_\phi(r,\varphi,z,t) = (\hat{E}_\varphi \cdot e^{i\omega t} + \hat{E}_\varphi^* \cdot e^{-i\omega t}) \cdot e^{-i\beta \cdot z}$$
$$E_z(r,\varphi,z,t) = (\hat{E}_z \cdot e^{i\omega t} + \hat{E}_z^* \cdot e^{-i\omega t}) \cdot e^{-i\beta \cdot z}$$

These complex functions depend only on the local position (r,φ,z) and the $*$ indicates the complex conjugate value.
Introducing the wave number k, the wavelength λ, the frequency ν the wave equations eq. 3 and eq. 4 become for the direction in z :

$$(\Delta + k^2 \cdot n^2) E_z = 0 \qquad \text{eq. 5}$$

$$(\Delta + k^2 \cdot n^2) H_z = 0 \qquad \text{eq. 6}$$

We write the Δ operator (Laplace) in cylindrical coordinates:

$$\Delta_{cyl} = \frac{1}{r} \cdot \frac{\partial}{\partial r}\left(r \cdot \frac{\partial}{\partial r}\right) + \frac{1}{r^2} \cdot \frac{\partial^2}{\partial \varphi^2} + \frac{\partial^2}{\partial z^2},$$

which we rearrange for our purposes in the following way:

$$\Delta_{cyl} = \Delta_{r,\varphi} + \Delta_z$$

The transversal *(r, φ)* and the longitudinal *(z)* component of the electrical field are separated by introducing the following expression

$$E_z = E_z(r,\varphi) \cdot E_z(z)$$

Applied to eq. 5 we obtain:

$$(\Delta_{cyl} + k^2 \cdot n^2) \cdot E_z(r,\varphi) \cdot E_z(z) = 0 \qquad \text{eq. 7}$$

With the additional relation:

$$\Delta(E_z(r,\varphi)\cdot E_z(z)) = E_z\cdot\Delta E_z(r,\varphi) + E_z(r,\varphi)\cdot\Delta E_z(z)$$

and with eq. 1 we can write:

$$E_z(z)\cdot(\Delta_{r,\varphi} - \beta^2 + k^2 n^2)E_z(r,\varphi) = 0$$

To reduce the writing and for simplification let's use:

$$k_{r,n}^2 = n^2k^2 - \beta^2$$

$$E_z(z)\cdot(\Delta_{r,\varphi} + k_{r,n}^2 n^2)E_z(r,\varphi) = 0$$

To fulfil the above equation and since $E_z(z)$ may have values unequal zero the second part of the equation above must be zero:

$$(\Delta_{r,\varphi} + k_{rn}^2)\cdot E_z(r,\varphi) = 0 \qquad \text{eq. 8}$$

On the further way to solve the differential equation eq. 8 we separate $E_z(r,\varphi)$ by using a statement of the type

$$E_z(r)\cdot E_z(\varphi)$$

Since the fibre has a rotational symmetry with respect to φ the expression $E_z(\varphi) = E_z(\varphi+2\pi)$ must be valid. This suggests to try the following statement:

$$E_z(\varphi) = e^{i\cdot p\cdot 2\cdot\pi\cdot\varphi},$$

whereby p is an integer and placing this into eq. 8 we get:

$$\Delta_{r,\varphi}(E_z(r)\cdot E_z(\varphi)) + k_{r,n}^2\cdot E_z(r)\cdot E_z(\varphi) = 0$$

or

$$\Delta_{r,\varphi}(E_z(r)\cdot E_z(\varphi)) = E_z(\varphi)\cdot\Delta_r E_z(r) - E_z(r)\cdot\frac{p^2}{r^2}\cdot E_z(\varphi)$$

or

$$E_z(\varphi)\cdot\left((\Delta_r - \frac{p^2}{r^2} + k_{r,n}^2)\cdot E_z(r)\right) = 0$$

$E_z(\varphi)$ is not necessary always zero and thus the bracket must be zero. As we will see later, it makes sense to multiply the content of the bracket with r^2:

$$(r^2\cdot\Delta_r - p^2 + r^2\cdot k_{rn}^2)\cdot E_z(r) = 0$$

Rewriting the Laplace operator with only those components which are only acting on the radial components we get:

$$\left(r^2\cdot\frac{\partial^2}{\partial r^2} + r\cdot\frac{\partial}{\partial r} + r^2\cdot k_{r,n}^2 - p^2\right)\cdot E_z(r) = 0$$

For cosmetic reasons we set $r\cdot k_{r,n} = x$ and $E_z(r) = y$ and obtain:

$$x^2\cdot\frac{\partial^2 y}{\partial x^2} + x\cdot\frac{\partial y}{\partial x} + (x^2 - p^2)\cdot y = 0 \qquad \text{eq. 9}$$

This is a differential equation with cylindrical functions and only for specific values of p it can be transformed into elementary functions.

This differential equation kept Mr. Bessel (1784-1895), Mr. Neumann (1798-1895) and Mr. Hankel (1814-1899) restless till they found a solution.

For reader working in the field of microwaves will know this kind of equation since it is also used to solve problems of wave propagation within electric waveguides. However, the difference to waveguides is, that fibre optics are non-conductive instead of conductive matter.

It is a long way to solve eq. 9 and we will illustrate just the main steps:
Out of the known 4 solutions (cylindrical function) we have to select that one which fulfils the demands of the physics laws.
For the cladding of the fibre we need a solution which is real. Therefore the modified Hankel function is applied
Since eq. 9 is homogenous (the right side is zero), also linear combinations of the solutions fulfil the equation. Fortunately the physical situation reduces the number of solutions.
The Neumann function has the property that it becomes infinity for $x\to 0$ or $r\to 0$. That means that the electrical field of the light would be infinite in the centre of the fibre which is not in agreement with the reality, thus this solution has to be disregarded.
The Bessel function shows finite values in the centre of the fibre. For larger values of x or r the Bessel function oscillate in a sine or cosine manner. In so far the Bessel-function is a suitable solution for the core.
For the cladding of the fibre we need in addition an attenuation of the field. Here the modified Hankel-function is a promising solution. However, for *x or r⟶0* the Hankel function becomes infinite. In fact that is not a problem since we need it only for the range $r \geq a$ (cladding).
Conclusion:
For the range $r \leq a$ (core) we apply the Bessel-function.
For the range $r \geq a$ (cladding) the Bessel-function is the choice.
It remains to find a solution at the boundary between core and cladding. The continuity conditions of the components of E and H fields of the light for the transition from core to cladding must be maintained. The Bessel and Hankel functions needs to be fitted to for $r = a$.

The solution will require the existence of so called transverse electromagnetic fields, which can be interpreted as modes of the fibre. As we already know from the Maxwell's equation an electrical field is accompanied by a magnetic field.

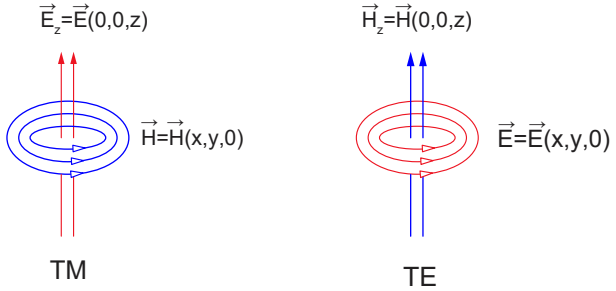

Fig. 5: Basic electromagnetic fields

The Fig. 5 show the fundamental E and H combination. Of course a lot of combinations of TM and TE exist. However,

Theory

we are interested only in such a mode which is propagating inside the single mode fibre. To achieve this, the general solution requires the fulfilment of the expression below:

$$1.5 < \frac{\pi d}{\lambda} \cdot \sqrt{n_{co}^2 - n_{cl}^2} \leq 2.405 \qquad \text{eq. 10}$$

In the above expression d is the diameter of the fibre core and λ the wavelength of the conducted light, n_{co} is the index of refraction of the core and n_{cl} that one of the cladding.

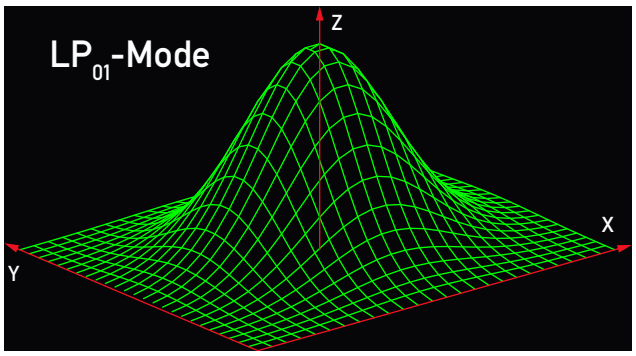

Fig. 6: Intensity distribution of the LP_{01} wave

In the following we want to know the diameter of a fibre for a singlemode (LP_{01}) transmission. We set the inner part of eq. 10 to *V(λ)*. For a core diameter d = 9 µm of an optical fibre we calculate *V(λ)* as function of the wavelength and plot the result in the graph of Fig. 7. The upper limit value of 2.405 and the lower limit value are drawn as lines in side the graph. All wavelength falling into this range will propagate as singlemode radiation along the fibre. Above the value of 2.405 the radiation propagates in multimode. The minimum wavelength for which the function V(λ) yields 2.405 is termed as cut-off wavelength and is in this example 1.100 nm.
The diameter of 9 µm has been chosen because of an important technical aspect. It is know, that a special kind of glass has absorption minima at 1.300 and 1500 nm, whereby the absorption at the longer wavelength is even less. For both cases the light will travel in singlemode, which is important for fast data transmission in telecommunication.

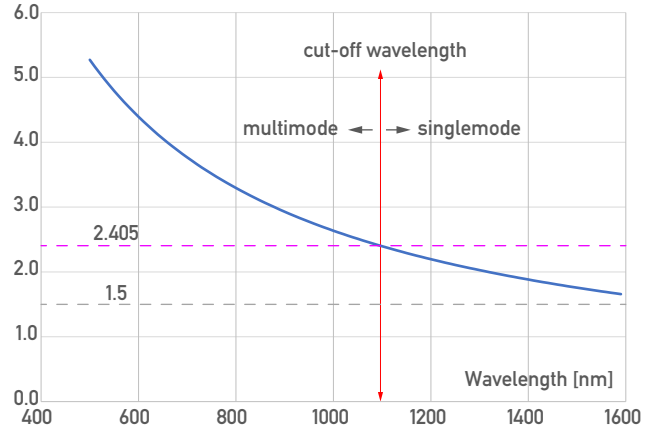

Fig. 7: V(λ) as function of the wavelength for a fibre with a core diameter of 9 µm

2.1 Coupling of light to fibre

How to get the light into a fibre. A beam of light needs to be launched into the core of a fibre whereby the core diameter is in the range of 4-10 µm which is comparable to the wavelength of light. To get a sufficient amount of light into the fibre, the beam of the light source has to be focused down to the diameter of the core.

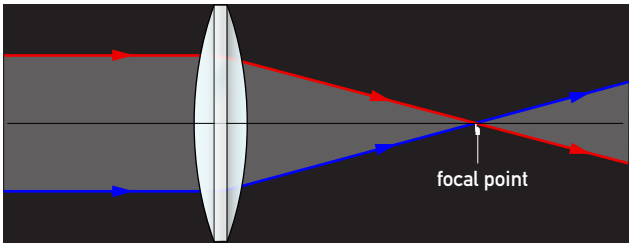

Fig. 8: Focusing of two beams according to geometrical optics

In reality either parallel light nor a focus with zero diameter does exists. Thus the geometrical optics should only be used to provide an overview.

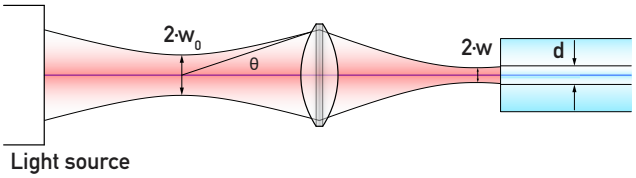

Fig. 9: Coupling light to an optical fibre

The Fig. 8 shows a more realistic illustration, instead of parallel beams, Gaussian beams with their respective beam waists are shown. To describe this reality in a more precise way we use the Maxwell's equations again. To do so, we again use the wave equation derived from the Maxwell equation:

$$\Delta\vec{E} - \frac{n^2}{c^2} \cdot \frac{\partial^2 \vec{E}}{\partial t^2} = 0$$

In this case we are only interested in the electrical field of the light since there are no interactions with magnetic dipoles in the propagation space.

Without restrictions the light would propagate as a spherical wave in all directions.

$$\vec{E} = \vec{E}(r) \text{ with } r^2 = x^2 + y^2 + z^2$$

When we consider the technically more important case of spherical waves propagating in the direction of z within a small solid angle we arrive at the following statement for the electrical field:

$$\vec{E} = \vec{E}(r,z) \text{ with } r^2 = x^2 + y^2 + z^2$$

In this case the solution of the wave equation provides electrical light fields which have a Gaussian intensity distribution over the cross-section, consequently called Gaussian beams. Similar to the solutions for the fibre, the Gaussian beams also exist in different modes depending on the implied boundary conditions. Such modes, especially the Gaussian fundamental mode (TEM_{00}) are generated by lasers. However,the light of any light source can be considered as the superposition of different Gaussian modes. The intensity of a particular mode of a non coherent light source is small with respect to the overall intensity of it. For laser the situation is different, here the total light power can be contained in one fundamental mode. This is the most outstand-

ing difference to ordinary light sources. How the Gaussian beams behave differently from geometrical beams we will show in the following.

A Gaussian beam always has a waist. The beam waist radius w is a results of the solution of the wave equation as follows:

$$w(z) = w_0 \cdot \sqrt{1 + \frac{z^2}{z_R^2}}$$

w_0 is the smallest beam radius at the waist and z_r is named as the Rayleigh length

$$z_R = w_0^2 \frac{\pi}{\lambda}$$

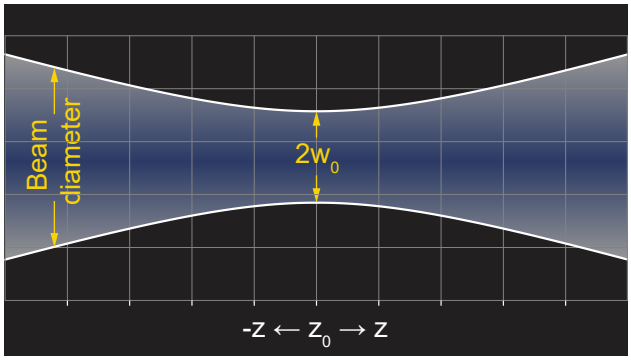

Fig. 10: Beam diameter as function of z of a Gaussian beam of a fundamental mode TEM_{00}

The Fig. 10 shows the course of the beam diameter of a Gaussian beam as a function of z. At the position $z = z_0$ the beam has the smallest beam waist. The beam waist size increases linearly with increasing distance. Gaussian beams are spherical waves thus a radius of curvature of the wave field to each point z can be attributed. This radius of curvature R (ROC) derived from the solution of wave equation is given by:

$$R(z) = z + \frac{z_r^2}{z}$$

This relation is illustrated in Fig. 16.

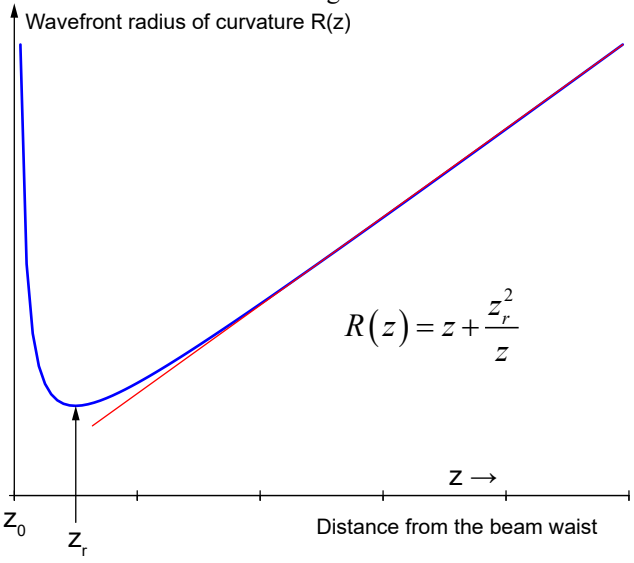

Fig. 11: The radius of curvature of the wave front as a function of the distance from the waist at z_0

The ROC shows a minimum for $z = z_r$. For smaller values of z the ROC increases and for $z=0$ it is infinite, that means the wave front is plane like for parallel waves. For higher values of z the radius of curvature increases linearly, indicated by the red line. This implies an important statement: a beam with infinite ROC (parallel beam) excists only in one point of the light wave, namely only in its focus. A not so strict interpretation defines a range for which the wave can be considered as parallel:

$$-z_r \le z \le z_r$$

The so defined Rayleigh range is shown in Fig. 12 as well as the far field ($z>>z_0$) divergence Θ is shown as well.

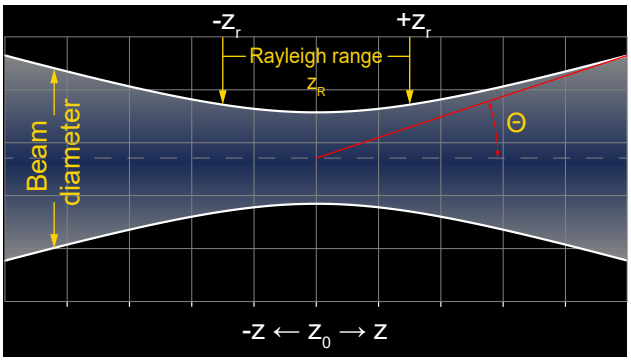

Fig. 12: Rayleigh range and far field divergence Θ

It should be mentioned, that the illustration of Fig. 12 does not reflect the real situation of a laser beam. The ratio of the Rayleigh range and the beam diameter is far apart from reality, but serves to explain these properties. To see how reality is, we consider, for example green laser pointer (532 nm) with a beam radius of $w_o = 1\ mm$ at the exit of the pointer. For the Rayleigh range $z_R = 2\ z_r$ we get:

$$z_R = 2 \cdot w_0^2 \frac{\pi}{\lambda} = 2 \cdot 10^{-6} \frac{3.14}{532 \cdot 10^{-9}} = 11{,}8\ m$$

That means that the ratio of the Rayleigh range to the beam diameter is 11.8 /0.002 which yields 5900, which is impossible to illustrate in a graph.

Coming back to the initial task, to treat the light waves as Gaussian waves and launch the light into the fibre. It is clear, that we need to focus the light by means of a lens in such a way that the beam waist of the focussed light is in the order of magnitude of the core diameter of the fibre. The following considerations shall give us an idea.

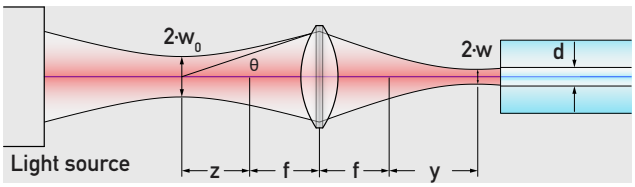

Fig. 13: Layout for the coupling optics

To get a maximum of power into the fibre a lens with a focal length of f is required to couple a Gaussian beam into a weak guiding step index fibre for the LP_{01} fundamental mode only. The radius at the waist is

$$w = \frac{w_0 \cdot f \cdot \theta \cdot}{\sqrt{w_0^2 + \theta^2 \cdot z^2}}$$

The position of the waist is:

Theory

$$y = \frac{z \cdot f^2}{z^2 + \left(\frac{w_0}{\theta}\right)^2}$$

Example: The beam of a laser pointer of 1.5 mm diameter and of 2 mrad divergence is focussed with a lens of 50 mm focal length with a distance of 2 m apart from the laser. We find:

$$w = \frac{1.5 \cdot 10^{-3} \cdot 0.05 \cdot 2 \cdot 10^{-3}}{\sqrt{2.25 \cdot 10^{-6} + 4 \cdot 10^{-6} \cdot (2 - 0.05)^2}} = 35.9 \mu m$$

$$y = \frac{(2 - 0{,}05) \cdot 2{,}5 \cdot 10^{-6}}{(2 - 0{,}05)^2 + \left(\frac{1{,}5}{2}\right)^2} = 1.1 mm$$

For this example the position y of the waist is 1.1 mm apart from the fibre entry face. The radius of the waist is 35.9 µm and the coupling efficiency for a 9 µm fibre will be miserable. To get a better performance the parameter z must be modified in such a way that the radius of the beam overlaps with the radius of the core.

2.2 Properties of laser diodes

Laser diodes are a specific class of lasers. They differ from other common lasers in two major aspects:

1. In conventional lasers the laser-active material (atoms, molecules or ions) are independent from each other as such and only distinct energy levels are involved in the laser process. This implies that in principle an energy level can be populated by an infinite number of atoms or molecules or ions. This is not the case with semiconductor lasers. Here a defined energy level can only be occupied by two active particles (electrons, Pauli principle). But in semiconductors, the wave functions of the involved atoms may overlap to form a common energy band. Thus for the laser process, the transition between the distribution of population in two energy bands instead of two energy levels must be taken into account. This is why laser diodes do not have an inherently defined emission wavelength.
2. The second important difference concerns the propagation of the laser light within the pn zone of the semiconductor. The spatial intensity distribution of the laser beam is defined by the laser medium and not by the resonator as it is the case for conventional lasers. This leads to a laser beam which has an elliptical instead of a round intensity distribution.

3. Photodiode

Semiconductor pn-transitions with a band gap of E_g are suitable for the detection of optical radiation if the energy E_p of the photons is equal or greater than the band gap.

$$E_p = \hbar\omega \geq E_g$$

In this case an incident photon can excite an electron to transfer from the valence band to the conduction band (Fig. 14).

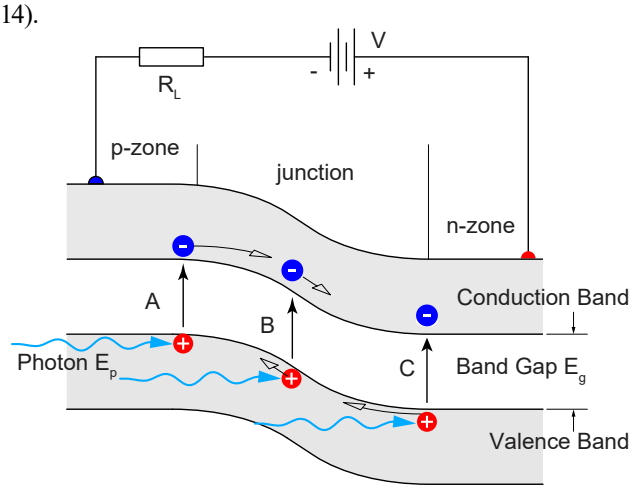

Fig. 14: Semiconductor with pn transition and absorption of an incident

In such a structure three general types of events occur:

A An electron of the valence band in the p-zone is excited by a photon and transferred into the p-zone of the conduction band and leaves a so called hole behind. Under the influence of the applied external electric field with voltage V, it will diffuse through the junction into the n-zone and contributes to the external current via the resistor R_L unless it recombines in the p-zone.

B If an electron of the junction is excited a photon the hole of the junction will migrate into the p-zone and the related electron into the n-zone. The drift of both charges through the junction causes a current flow. The duration of the so generated pulse depends on the drift speed and on the length of the junction.

C The case is similar to case A. The electron is lifted into the conduction band and related the hole migrates due to the presence of the external field into the p-zone or recombines in the n-zone.

Only electrons which are located inside the junction (case B) or near the boundary of the junction (area of diffusion, case A and C) contribute to the external current by the excitation of an incident photon. All other events will recombine within their area. In the best possible case one elementary charge q is created for each incident photon. However, in average not every photon will create such a current pulse with load q. To quantify the conversion efficiency we define the production or conversion rate G and the average photocurrent $\langle i_{Ph} \rangle$ is defined as follows:

$$\langle i_{Ph} \rangle = q \cdot G$$

One photon has an energy of $E=h \cdot \nu$, an incoming light energy of P_0 contains a number n photons given by:

$$n = \frac{P_o}{h \cdot \nu}$$

But only a fraction of photons are absorbed inside the junction and converted into current pulses. This fraction may be termed as

$$\eta \cdot P_0 ,$$

where η is called the ***quantum efficiency***. With this definition we write the expression for the number of generated current pulses or the production as:

$$G = \frac{\eta}{h \cdot \nu} \cdot P_0$$

and thus the average photo current:

$$\langle i_{Ph} \rangle = \frac{\eta \cdot q}{h \cdot \nu} \cdot P_0$$

It will be observed that there is already a current flowing although no photons entering the detector. This undesired current is called „dark“ current and has four main reasons:

1. Diffusion current, it is created because of statistical oscillations of the charge carriers within the diffusion area.
2. Regeneration or recombination current, it is generated by random generation and annihilation of holes.
3. Surface currents, which are hardly avoidable since the ideal insulator does not exist.
4. Avalanche currents appear at high electrical field strengths, if a high voltage is applied to the photodiode.

All these effects contribute to the dark current i_D in a way that the characteristic curve of the diode can be expressed as follows:

$$i = i_s \left(e^{\frac{q \cdot U_D}{kT}} - 1 \right) - \langle i_{Ph} \rangle = i_D - \langle i_{Ph} \rangle$$

This current i passes the load resistor R_L and creates the voltage drop U_a, which is linear to the photo current.

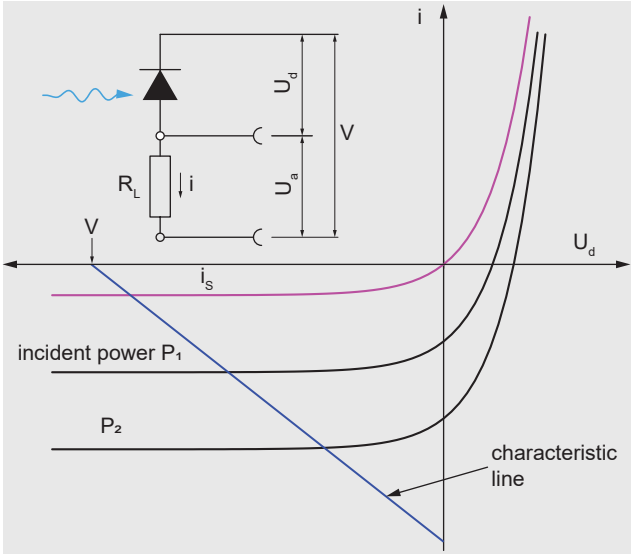

Fig. 15: Characteristic line of a photodiode in the photoconductive mode

$$i = i_s \left(e^{\frac{q}{kT} \cdot U_d} - 1 \right) - \langle i_{Ph} \rangle = \frac{U_a}{R_L}$$

A good detector for optical communication technology is very fast (up to the GHz range) and has a high quantum efficiency for a high sensitivity. Depending on the desired wavelength range either a silicon or a germanium based semiconductor is applied. Within the experiment a wavelength of 810 nm will be used we will focus on Si detectors, however most properties are transferable to Ge or InGaAs detectors.

2.3 Ge and Si PIN-diodes

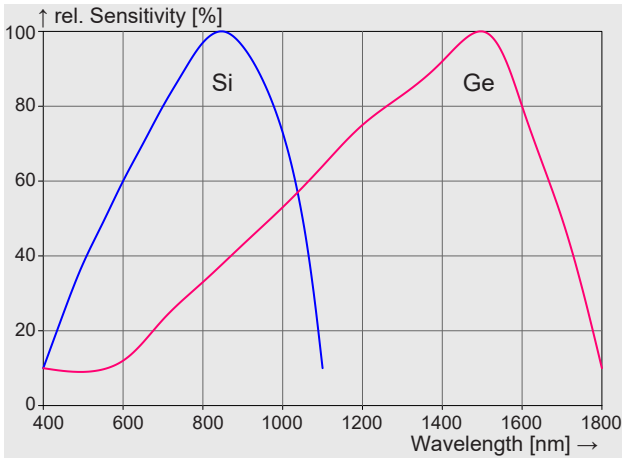

Fig. 16: Relative sensitivity for Si and Ge photodetector

To absorb a photon, its energy has to fit into the band structure of the used material that means:

$$E_{ph} = h\nu = h\frac{c}{\lambda} \geq E_G$$

For large wavelengths (lower photon energy) the energy of the photon may not be sufficient to excite and transfer the electron over the band gap. At a higher photon energy (lower wavelength) electrons may be lifted into a band gap above the conduction band and cannot be absorbed. Unfortunately there are currently no photodetectors available which covers the entire spectrum of light. Thus the applied light source decides which kind of detector material suits best. For wavelengths above 1 µm up to 1.5 µm Germanium or InGaAs is recommended. Below these values Silicon detectors are commonly used. In this experiment we use a laser diode with a wavelength of 810 nm. That is why a silicon detector is used and to achieve a high quantum efficiency PIN detector instead of a PN detector been chosen. Compared to a detector with a simple pn-layer this type of detector has an intrinsic layer (or undoped layer) inserted in between the p- and n-layer, therefore the name PIN-diode.

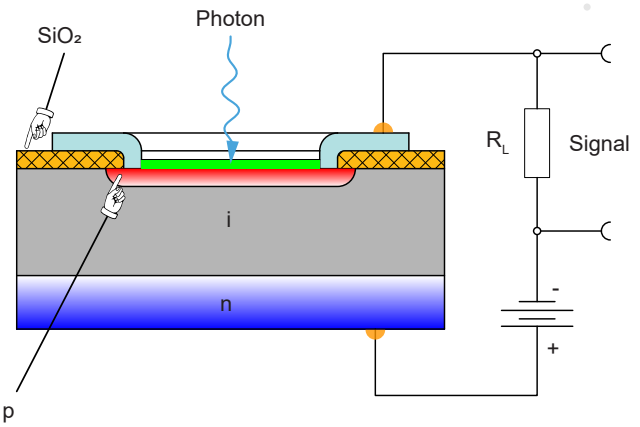

Fig. 17: Structure of a PIN detector

Such an i-layer enlarges the pn barrier layer which increases the probability of absorption of a photon and the related generation of a current pulse and improves the quantum efficiency η which can be expressed as:

$$\eta = (1-R)\left(1-e^{-\alpha d}\right)e^{-\alpha d_p}$$

R stands for the Fresnel reflection at the detector's surface for the incident photons, α is the absorption coefficient, *d* the thickness of the intrinsic zone and d_p the thickness of the p-layer. By coating the detector's surface on the upper side of the p-layer with an anti reflection coating the value for *R* can be reduced to less than 1%. The value of $\alpha \cdot dp$ is very small compared to 1 ($\alpha \cdot dp \ll 1$), which suggests to increase the thickness of the intrinsic layer as large as possible to obtain a high quantum efficiency. However, this would increase the drift time and thereby reduces the maximum frequency of the detector. A compromise between high quantum efficiency and high limiting frequency has to be made.
In this experiment a PIN-Si-photo diode of type BPX61 made by OSRAM is used. It has the following characteristic parameters.

Quantum efficiency η at 850 nm	90 %
Rise time $\tau_r = 2.2 \cdot R_L \cdot C_j$ 10%-90% at $R_L = 50\,\Omega$ and $U_d = 10V$	1.7 ns
Capacity C_j at U_d =	
0 V	73 pF
1 V	38 pF
10 V	15 pF
dark current i_d at $U_d = 10V$	2 nA
Photosensitivity at $U_d = 5V$	70 nA/lx

3.0 Experiments

3.1 Experimental set-up

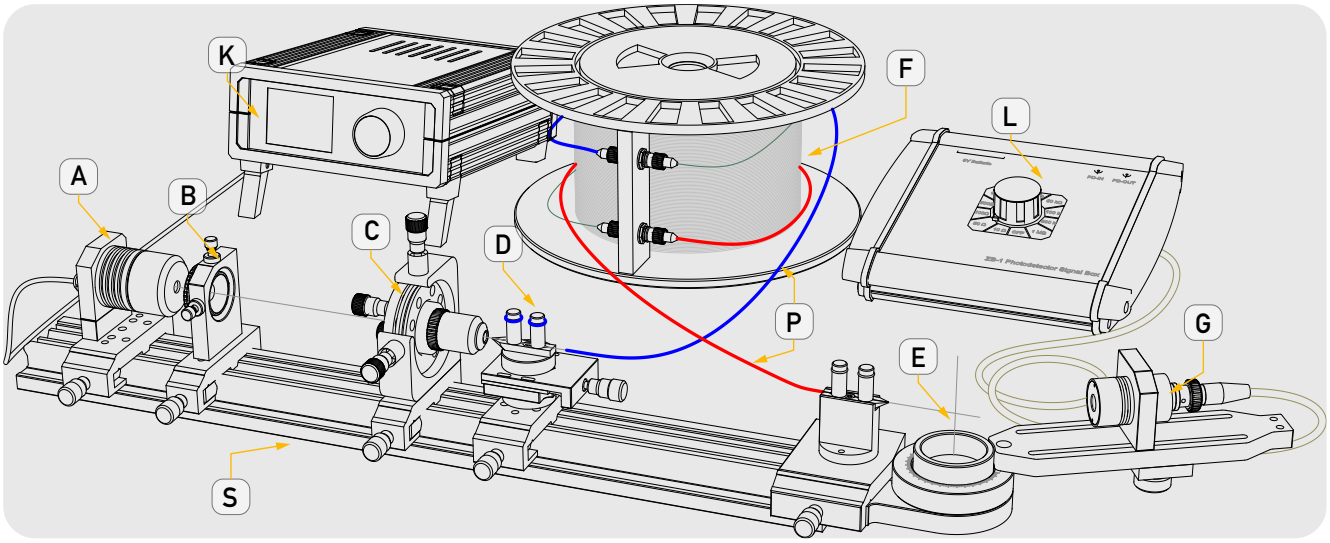

Fig. 18: Experimental set-up with fibre

3.2 Description of the components

A Diodelaser

The pump laser diode is mounted onto a Peltier element to control the operating temperature in a range of 10 .. 50 °C. The output power is 1 Watt at a wavelength of 810 nm. This device emits invisible light which can be hazardous to the human eye. The operators of the diode laser module have to follow the safety precautions found in IEC 60825-1 “Safety of laser products Part 1: Equipment classification, requirements and user’s guide” when connected to the controller. The diode laser (LD) is connected via a 15 pin SubD HD connector (CN) to the controller MK1. Inside the connector an EPROM contains the data of the laser diode and when connected to the controller, these data are read and displayed by the controller.

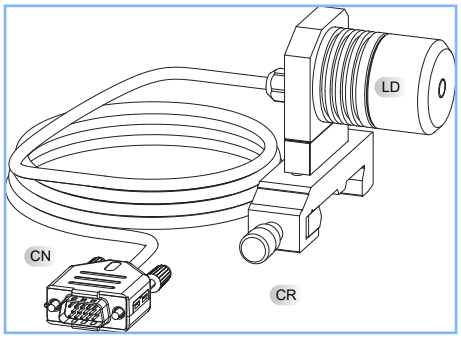

Fig. 19: Diode laser module (DL)

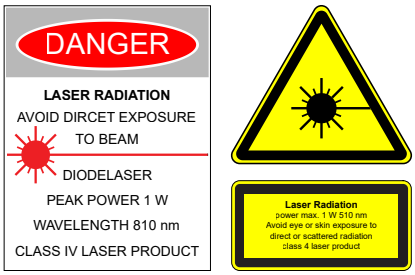

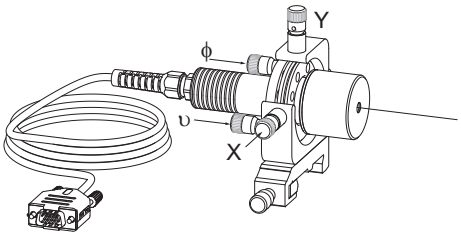

Fig. 20: Diode laser module after revision 2020

Theory

B. Collimator

A high precision aspheric glass lens is mounted into a click holder (A) which is inserted into the XY adjuster (XY). By means of two fine pitch screws the collimator can be adjusted accordingly.
When a diode laser with adjustment screws is provided (Fig. 20), the collimator comes without adjustment screws (Fig. 22).

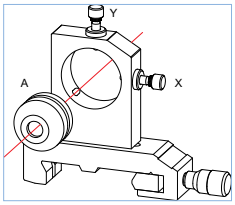

Fig. 21: Module Collimator (CO)

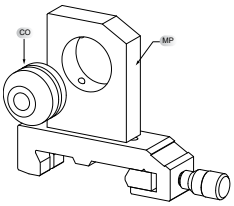

Fig. 22: Module collimator after version 2020

C. Focussing Optic

A microscope objective (x20) is used to focus the light into the fibre. Four precise fine pitch screws of repetitious accuracy allowing the translative (X,Y) and azimuthal (υ,φ) adjustment. The pitch of the screws is 250 µm.

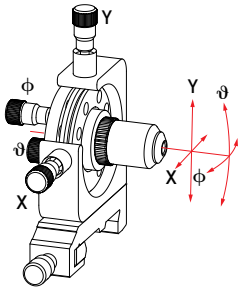

D Translation stage with fibre holder

A translation stage with a travel range of 5 mm is mounted to a 30 mm carrier. On top of it a fibre chuck with an inlaying groove for the fibre. Two magnets are attached to keep the fibre firmly inside the groove.

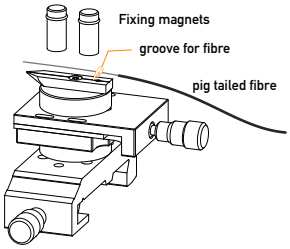

E. Fibre Goniometer

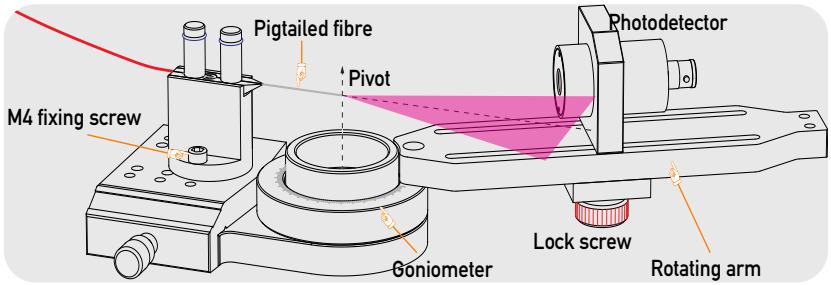

The fibre goniometer (E) consists of the fixed part which is attached at the end of the optical rail (S) with a carrier. On top of the carrier a fibre holder is mounted. For some experiment this holder needs to be removed by unscrewing the M4 fixing screws. The length of the pigtailed fibre is chosen in such a way that the exit of the fibre lies within the pivot. A rotating arm is fixed to the goniometer and carries a movable mounting plate to accommodate the photodetector. The mounting plate can be moved along the arm when loosening the lock screw and locked in the desired position.

F. Drum with 1000 m multimode fibre

A drum carries 1000 metres of a multimode fibre with a fibre core diameter of 50 µm and a cladding of 125 µm. The fibre ends are terminated by ST connectors which are connected to ST fibre panel jacks. The provided pigtailed fibre are bare on one side and terminated by an ST connector on the other end. Within the experiment the preparation of the fibres, like stripping and cleaving are trained. This is performed with the bare end of the fibre pigtails and does not effect the 1000 m long main fibre. Furthermore multiple fibre drums can be connected in series to study the effect of longer fibres.

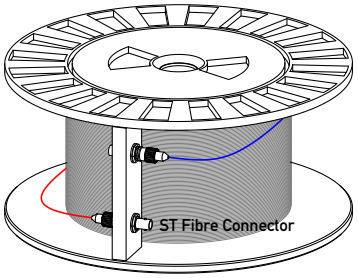

G. Si PIN photodetector module (PD)

A Si PIN photodiode is integrated into a 25 mm housing with two click grooves (PD). A BNC cable and connector is attached to connect the module to the photodetector signal box ZB1. The photodetector module is placed into the mounting plate (MP) where it is kept in position by three spring loaded steel balls.

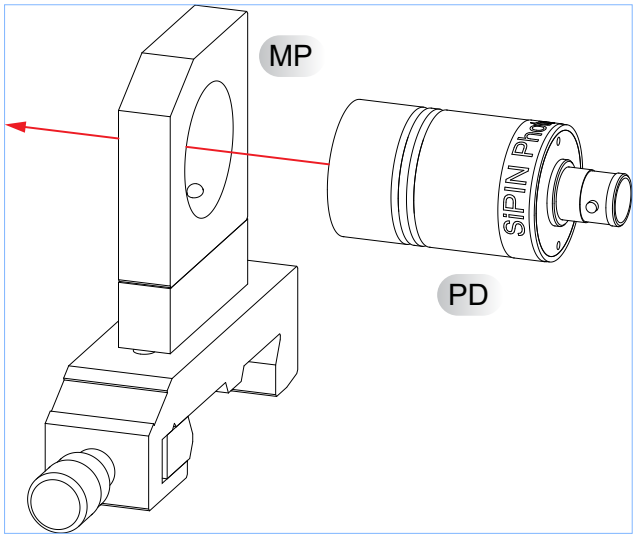

Fig. 23: Photodetector module

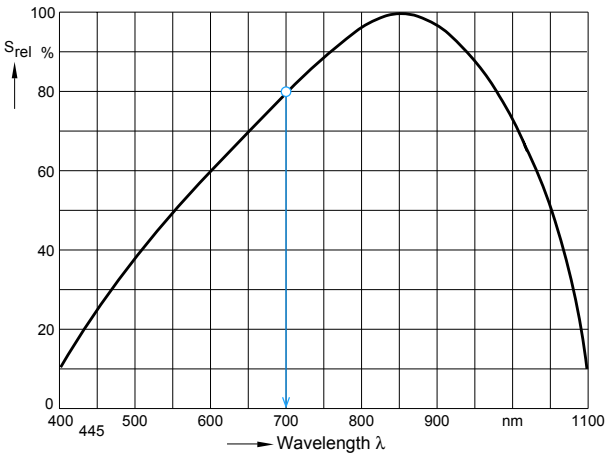

Fig. 24: Sensitivity curve of the BPX61 photodiode

Parameter	symbol	value
Rise and fall time of the photo current at: R_L=50 Ω, V_R=5V, λ=850 nm and I_P=800 µA	t_r, t_f	20 ns
Forward voltage I_F = 100 mA, E = 0	V_F	1.3 V
Capacitance at V_R = 0, f = 1 MHz	C_0	72 pF
Wavelength of max. sensitivity	λ_{Smax}	850 nm
Spectral sensitivity S~10% of S_{max}	λ	1100
Dimensions of radiant sensitive area	L x W	7 mm²
Dark current, V_R = 10 V	I_R	≤30 nA
Spectral sensitivity, λ = 850nm	$S(\lambda)$	0.62 A/W

Table 1: Basic parameters of Si PIN photodiode BPX61

L. Photodetector Signal Box ZB1

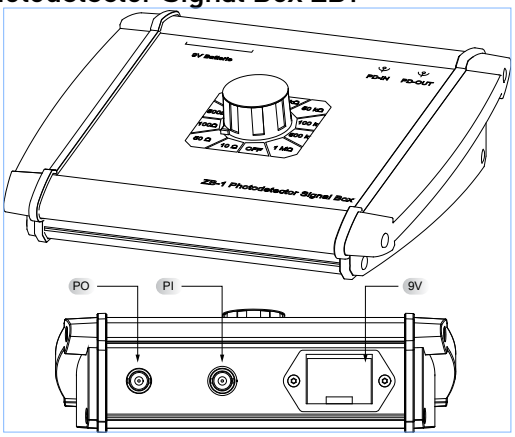

Fig. 25: Photodetector Signal Box ZB1

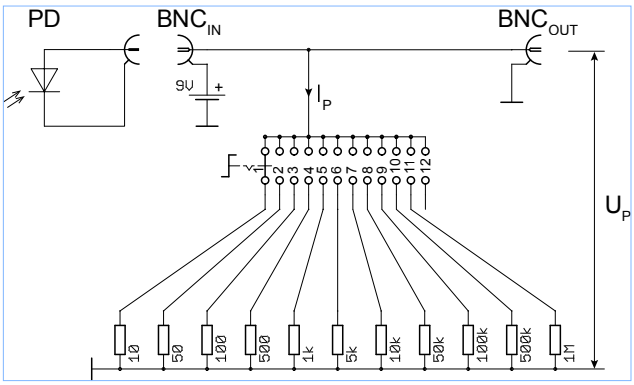

Fig. 26: Signal box schematic

The signal box contains a resistor network and a replaceable 9V battery and is prepared to accept all kind of photodiodes provided they are connected to the BNC input (PDIN) as shown in the schematic of Fig. 26. At the output (PDOUT) of the signal box a signal is present which is given by the following equation:

$$I_P = \frac{U_p}{R_L}$$

I_P is the photo current created by illuminating the photodiode with light.
U_p is the voltage drop across the selected load resistor R_L.
To convert the measured voltage into a respective optical power we have to make use of the spectral sensitivity $S(\lambda)$ [A/W] which depends on the wavelength of the incident light according toFig. 24. The detected optical power P_{opt} in Watt can be given as:

$$P_{opt} = \frac{I_p}{S(\lambda)}$$

Assuming a wavelength of 700 nm we take the value of S_{rel} from Fig. 24 as 0.8 and subsequently the value of S(λ=700 nm) is 0.62 x 0.8 = 0.496
If we measuring a voltage U_m of 5V with a selected resistor R_L of 1K the optical power will be

$$P_{opt} = \frac{I_p}{S(\lambda)} = \frac{U_p}{R_L \cdot S(\lambda)} = \frac{5}{1000 \cdot 0.496} = 10mW$$

It must be noted that the measured power is correct only if the entire light beam hits the detector. Based on the selected load resistor the sensitivity will be high for higher resistors but the rise and fall time will be longer. For fast signals a

low resistor should be used, however the sensitivity will be lower.

3.2.1 Digital Diode Laser Controller

Fig. 27: Digital Diode Laser Controller MK1

The laser diode module is connected via the 15 pin HD SubD jacket (LD). The controller reads the EEPROM of the laser diode and sets the required parameter accordingly. The MK1 is powered by an external 12V/ 1.5 A wall plug supply. A USB bus allows the connection to a computer for remote control. Furthermore firmware updates can be applied simply by using the same USB bus.
The MK1 provides an internal modulator which allows the periodic switch on and off of the diode laser. A buffered synchronisation signal is available via the BNC jacket (MOD). Furthermore the duty cycle of the modulation signal can be varied in a range of 1...100 % to enable the measurement of thermal sensitivity of the optically pumped laser crystal.
The controller is equipped with industrial highly integrated circuits for the bipolar Peltier cooler (Maxim, MAX 1978) as well as for the injection current and modulation control (iC Haus, iC-HG) of the attached laser diode. Further detailed specifications are given in the following section of the operation software.

3.2.2 Diode laser controller screens

When the external 12 V is applied, the controller starts displaying the screen as shown in the figure below.

Fig. 28: Start screen

Laser Safety

The first interactive screen requires the log in to the device since due to laser safety regulations unauthorized operation must be prevented. In general this is accomplished by using a mechanical key switch. However, this microprocessor operated device provides a better protection by requesting the entry of a PIN.
After entering the proper key the next screen is displayed and the system is ready for operation.

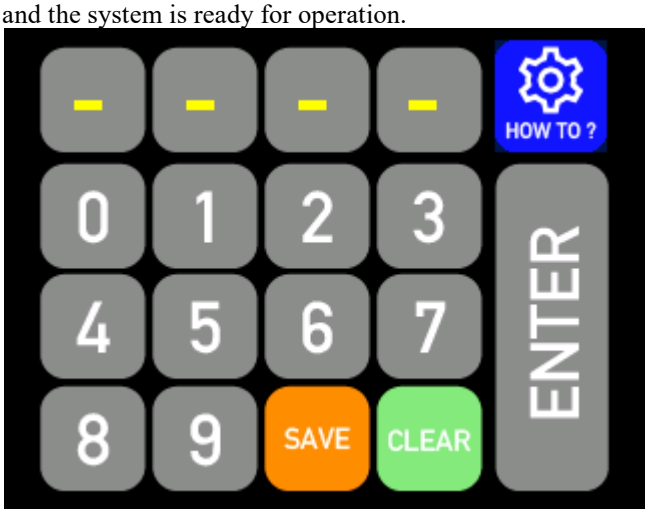

Fig. 29: Authentication screen

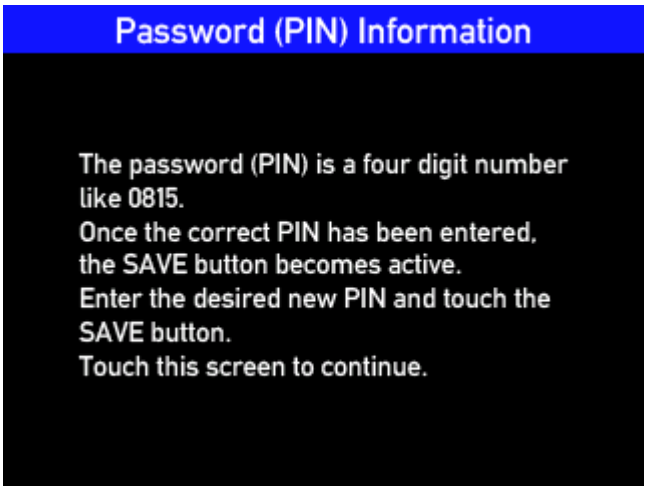

Fig. 30: Information for the password

Main Screen

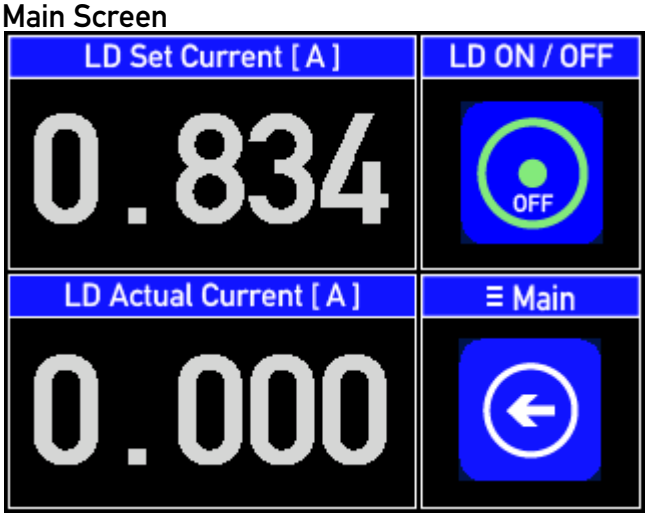

For immediate “Laser OFF” just tap the yellow button. To set the injection current simply tap the injection current dis-

play and turn the settings button (SET).

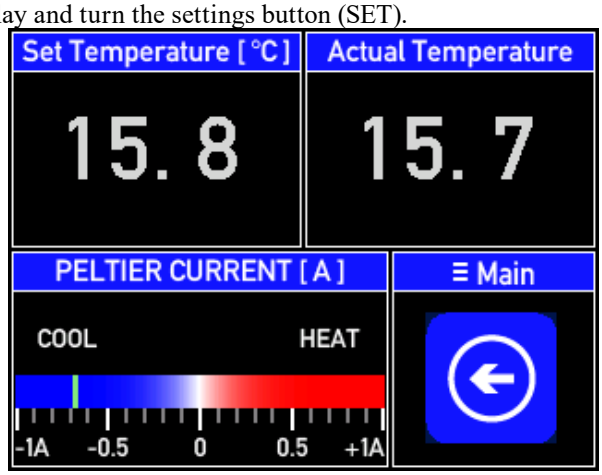

The same is true also for the "Set Temperature" section. When in operation and connected to the laser diode the actual temperature is shown in the "Actual Temperature °C section. Furthermore the actual current of the Peltier element is shown in such a way, that cooling or heating of the element can be observed.

Information screen

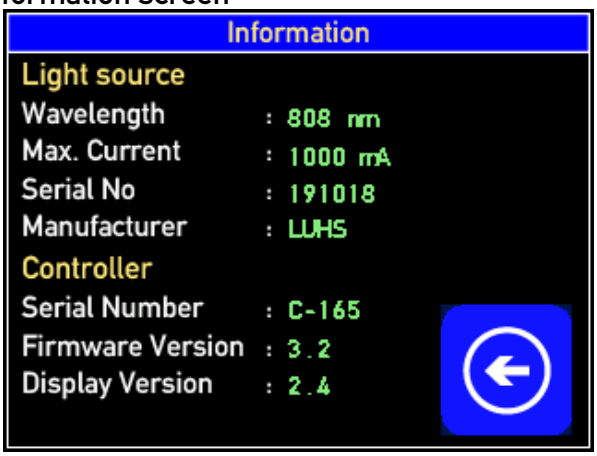

When tapping the Device Info button of the main screen this screen comes up. It again reads and displays the information stored in the EEPROM of the attached diode laser. If an entry exceeds the maximum or minimum limit value retrieved from the EEPROM of the attached diode laser the entry is reversed to the respective minimum or maximum value.

Modulation settings

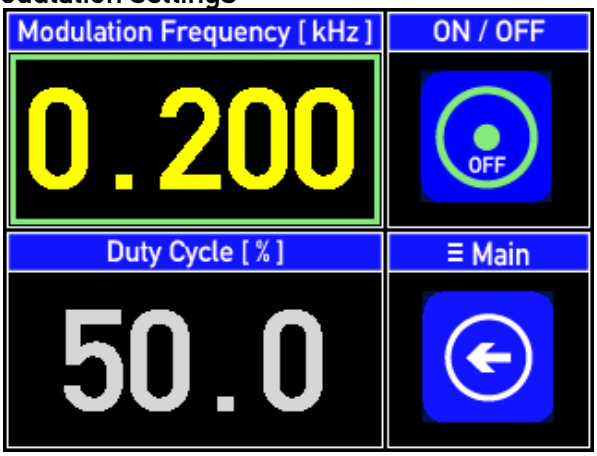

The diode laser can be switched periodically on and off. This is for a couple of experiments of interest. By tapping the display of the modulation frequency the entry is activated. Turning the settings knob will set the desired frequency value. The modulation becomes active, when the Modulator ON/OFF button is tapped.

Duty Cycle settings

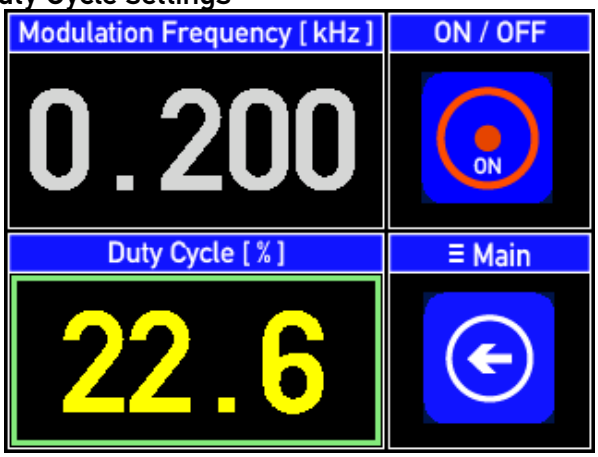

For some experiments it is important to keep the thermal load on the optically pumped laser crystal as low as possible or to simulate a flash lamp like pumping. For this reason the duty cycle of the injection current modulation can be changed in a range of 1...100 %. A duty cycle of 50% means that the OFF and ON period has the same length. The set duty cycle is applied instantly to the injection current controller.

Overheating warning

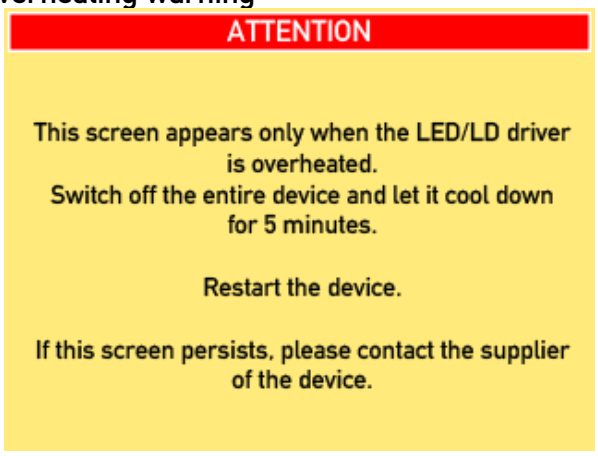

This screen you should never see. It appears only when the chip of the injection current controller is over heated.
Switch of the device, wait a couple of minutes and try again.
If the error persists please contact your nearest dealer.

This screen is self explanatory and appears either when no laser diode is connected or the data reading from the EEPROM is erroneous.

4.0 Preparation of the fibre

Before the fibre can be used it has to be prepared in such a way that the input as well as output surfaces are perpendicular to the core axis and of best optical quality. This is achieved by controlled breaking of the fibre using a one step fibre cleaver and breaker. Before this can be done the plastic buffer coating has to be removed, which is done by using so called Miller's pliers. It is a kind of cable stripper however for a thin cable of 125 µm.

Fig. 31: Miller's pliers

The pliers must be adjusted that the closed pliers does not injure the cladding glass of the fibre when stripping the plastic buffer. The pliers are coming pre-adjusted and if necessary the fixing screw of the diameter set screw is loosened and the diameter set screw is aligned.
After the plastic buffer has been stripped the fibre is ready to be cleaving and breaking.
For this purpose a cleaving and breaking tool is used. The following shows the operation of the Fitel's S315. Depending on availability the experiment may come with Fujikura CT02 or Sumitomo FC-6S cleaver. Although the latter one looks a bit different, the procedure is the same.

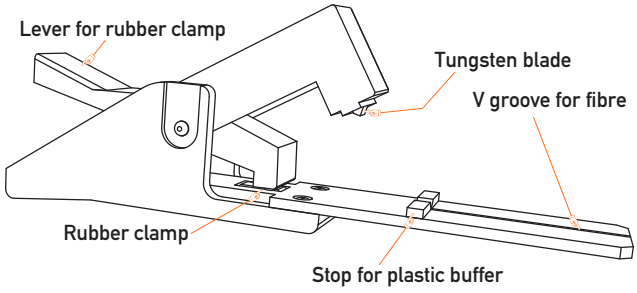

Fig. 32: Fibre cleaver and breaker

From the fibre a length of 25 mm of the plastic buffer is removed. The rubber clamp lever is pushed down to open the clamp. The fibre is placed set into the V - groove whereby the fibre end is inside the clamp the remaining plastic coating butts against the stopper.

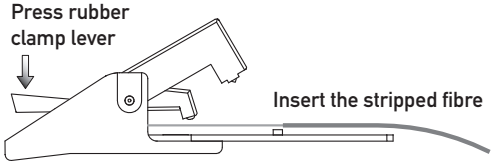

Fig. 33: First step: Insert the fibre

Press the lever as shown in Fig. 49 and insert the fibre.

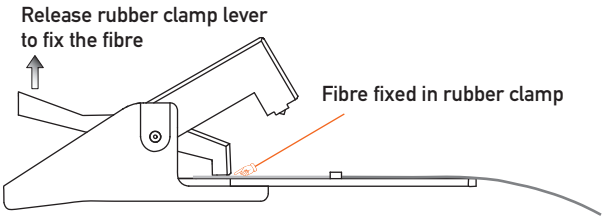

Fig. 34: Second step: Fix the fibre

Releasing the rubber clamp lever fixes the fibre inside the rubber clamp.

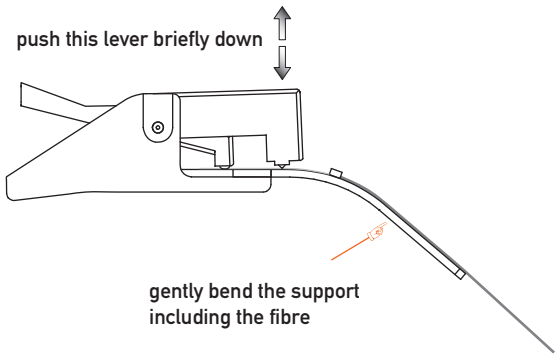

Fig. 35: Third step: cleaving (scratching) the fibre

Gently bend the support including the fibre and push briefly the cleaver blade onto the fibre, the fibre will break.

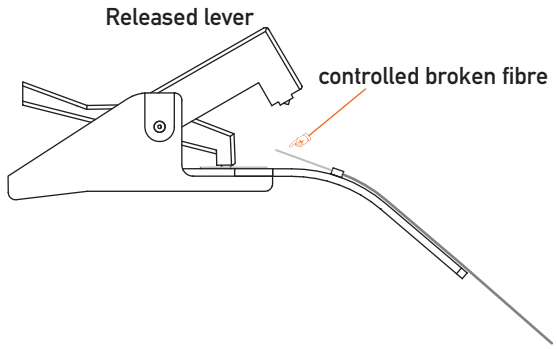

Fig. 36: Final phase: Remove the ready fibre from the cleaver.

Fig. 37: The fibre cleaver FC-62. The operating manual is attached as last 4 pages

Attention: Remove the residual splint of the fibre from the rubber clamp and deposit into the provided fibre scrap can to avoid that these parts may enter and injure the human body.

4.1 Properties of the laser diode

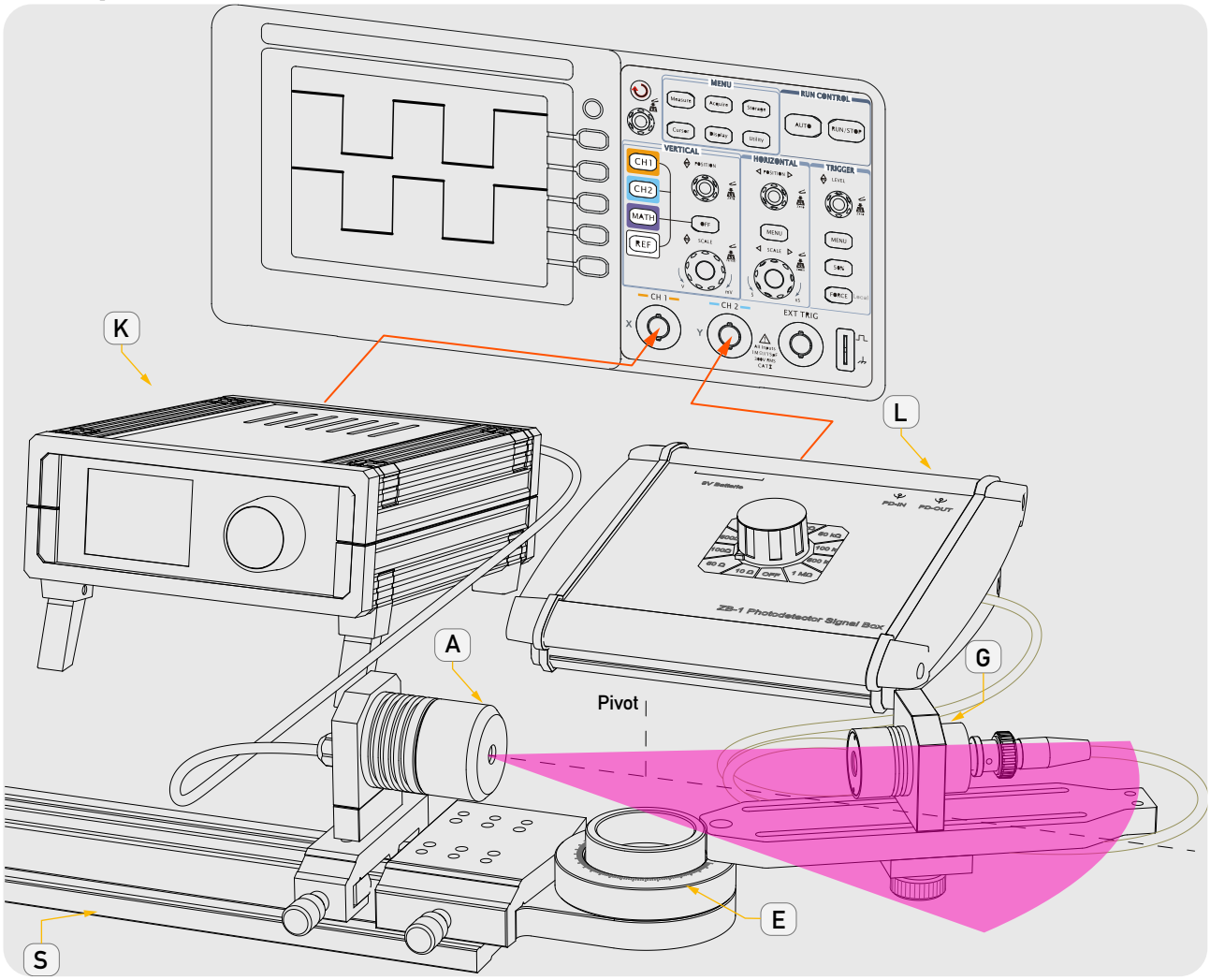

Fig. 38: Setup for the measurement of the spatial intensity distribution and the output power

With the above shown set-up two basic properties of the laser diode is measured. These are (A) the spatial intensity distribution and (B) the output power versus the injection current and diode laser temperature.

For this reason the laser diode module (A) moved as close as possible to the rotation joint of the goniometer (E) to keep the distance to the pivot as short as possible. To eliminate the influence of undesired environmental light on the measurement, the injection current of the laser diode is modulated by switching the controller MK1 into modulation mode. The output of the photo diode signal box is connected to one channel of an oscilloscope. This channel is switched to the „AC“ mode since we are only interested in the amplitude of the modulated signal to eliminate environmental light which otherwise may falsify the measurement.

Within the same set-up, but with the detector set to 0^0 to the laser diode, the output power is measured as a function of the injection current and the temperature.

If a spectrometer is available, even the dependence of the wavelength on the temperature and the injection current may be measured in addition.

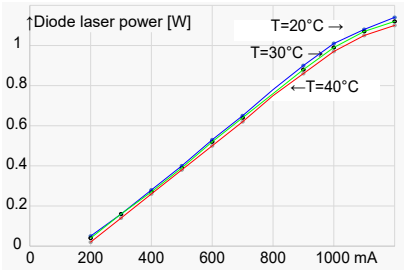

Fig. 39: Output power versus injection current

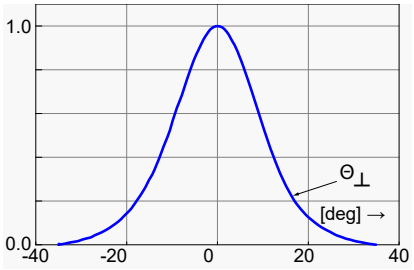

Fig. 40: Laser diode angular power distribution

Please note that the graphs of Fig. 39 and Fig. 40 are samples do not necessarily reflect real measurements.

4.2 Measurements with the fibre

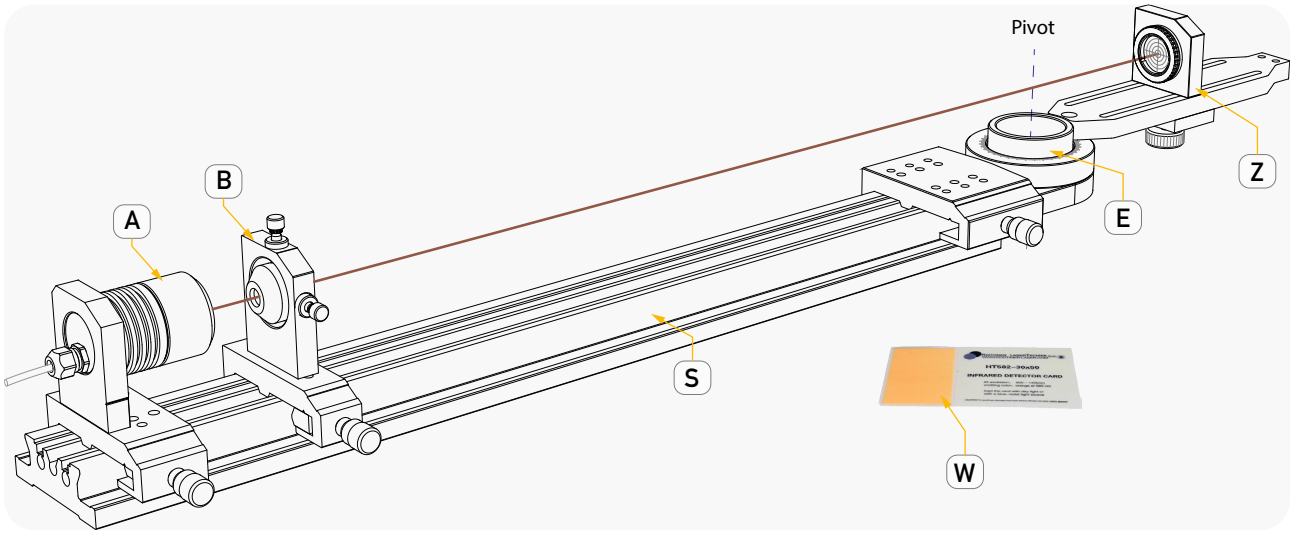

Fig. 41: Alignment of the diode laser

The diode laser emits a wavelength of 810 nm and can hardly be seen by the human eye, thus an infrared converter card (W) is provided which converts the radiation into a visible spot on a card when hit by the 810 nm radiation. This is a useful tool for the first alignment of the diode laser as shown in Fig. 41. The goniometer is set to 0 degree and the collimator (module B) is placed in front of the diode laser (A) so that an almost parallel laser beam is formed. With the fine pitch adjustment screws of module the collimator the laser beam is centred on the crossed hair target. This can also be checked by using the IR converter card.

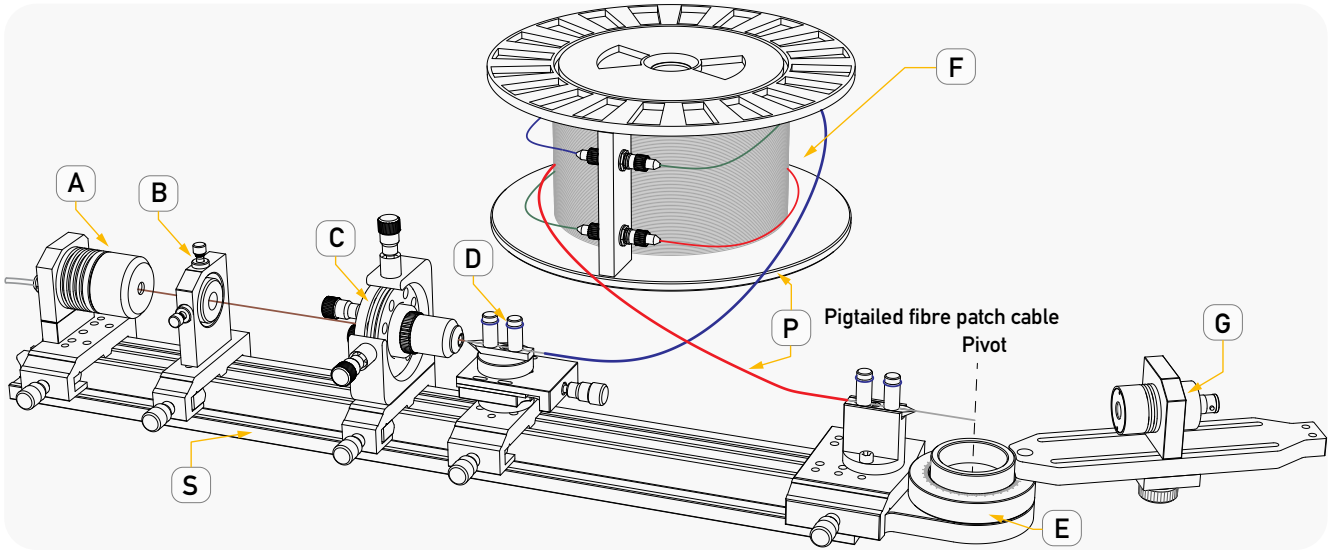

Fig. 42: Adding the next components

As next component the module C is placed onto the optical bench. Its distance to the collimator (B) is not critical since the laser beam is aligned in the previous step as almost parallel.

As next, the translation stage with the fibre chuck (D) without the fibre is set onto the rail at a distance of about 10 mm apart from the microscope objective of module C.

A pigtailed fibre patch cable (P) is connected to the fibre drum (it does not matter if exit or entry of the 1000 mm fibre). The bare end of the fibre is stripped and cut carefully mounted to the fibre chuck of module D and fixed by the two magnets. The same is performed for the pigtailed fibre patch cable which is attached to the fibre chuck of the goniometer module (E).

The photodetector (G) is set into the mounting plate of the rotation arm of the goniometer.

After connecting the laser diode to the controller and the photodetector to the signal box an oscilloscope is required to display and measure the signals. However, at first the focussing microscope objective of module C needs to be aligned for optimal coupling efficiency. For this purpose the photodetector is moved as close as possible to the fibre exit and if not already done, the goniometer is turned to its zero position.

The signal box is switched to a high shunt resistor (100 k or higher) and the output of the signal box is connected to the first channel of the oscilloscope. The modulator output of the diode laser controller is connected to the second channel and serves as trigger source.

The diode laser is set to its maximum power and the modulation frequency is set to 88 Hz at 50% duty cycle and after that the diode laser is switched on. One should already detect a small quantity of modulated laser light at the exit of the fibre which will be observed on the oscilloscope. Now further alignment of the fibre starts. While observing the amplitude on the oscilloscope one gently turns the adjust-

ment screws of the adjustment holder (E) for maximum amplitude as shown on the oscilloscope. If there is no further improvement the distance between the fibre and the microscope objective is changed by turning the set screw of the translation stage.
At the each new position the microscope objective is aligned again for maximum amplitude. At the optimum coupling the injection current of the diode laser should be to be reduced to avoid the saturation of the detector. The strong emission of the fibre can be observed on the IR converter card. The adjustment steps are repeated until no more coupling efficiency is obtained.

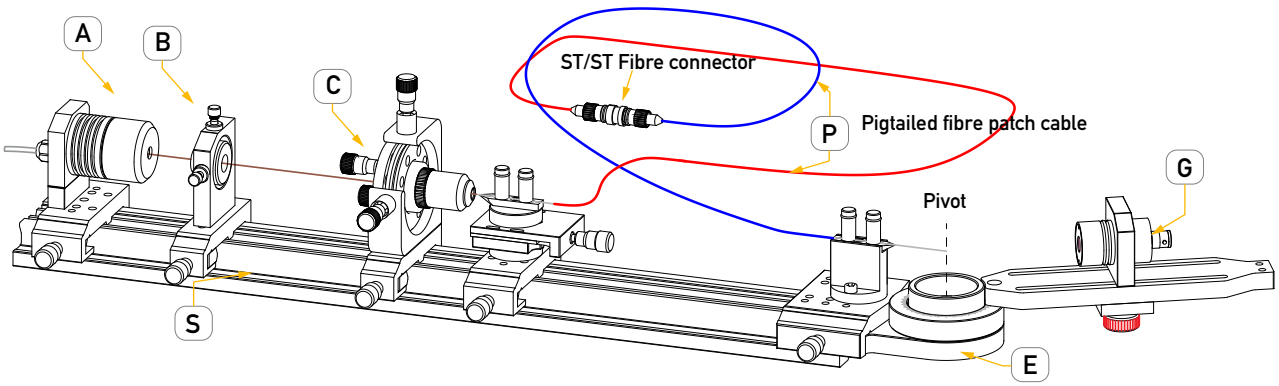

Fig. 43: Measurements without the long fibre

In order to measure the losses of the long fibre the measurement of a short fibre properties are carried out by using a connector which connects the pigtailed fibre. The output power as well as rise times are measured and compared to the measurements with the long fibre.

4.2.1 Measure the numerical aperture

The rotating arm of the goniometer (E) carries the photodetector which is used is used to measure the angle resolved intensity distribution. It makes sense to modulate the laser light to eliminate noise from external light sources. This allows also to detect small intensities which extends the measurable angle range.

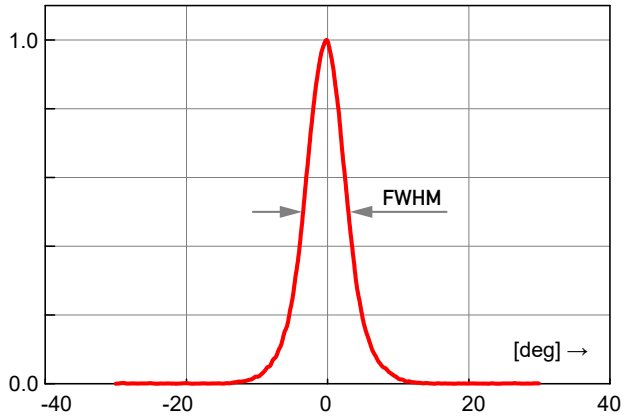

Fig. 44: Angle resolved intensity distribution of the multimode fibre (example)

4.2.2 Transit time measurement

Another very interesting experiment is the measurement of the time the light needs to pass the fibre.

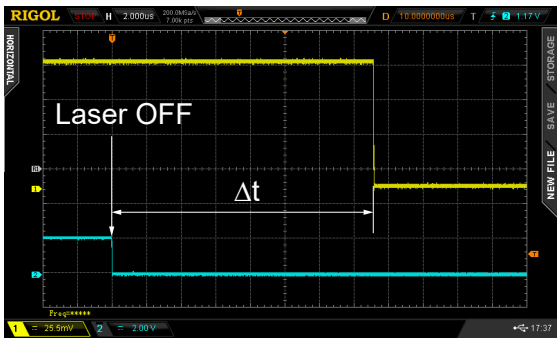

Fig. 45: Oscilloscope screen showing as lower trace (blue) the injection current of the diode laser and the upper one the signal of the light intensity at the exit of the fibre.

The facility to modulate the injection current of the diode laser makes it possible to measure the time of flight τ_{Light} of a laser pulse via 1000, 2000 or 3000 m of fibre. With the known length of the fibre even the speed of light can be determined and the index of refraction of the fibre calculated. The transit time through the fibre with a length of L and an index of refraction of n_{eff} can be calculated as follows:

$$\tau_{Light} = \frac{L}{c} \cdot n_{eff} = \frac{1000}{3 \cdot 10^8} \cdot 1.45 \approx 4.8 \mu s$$

The above value is obtained for a length of the fibre of 1000 metres only.

5.0 Laser safety remarks

The experimental set-up contains a laser which is only suitable for laboratory or educational applications.
With the individual modules in the assembled state, laser radiation (semiconductor laser) can be produced at 810 nm with a maximum power of 1 W.
The complete assembled laser is therefore a product which exhibits the power characteristics of a Class 4 laser.

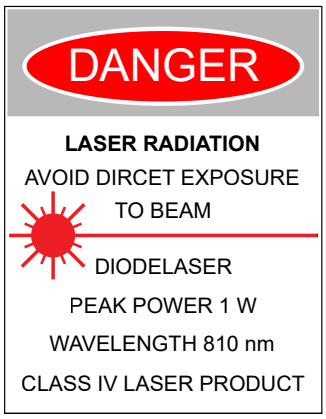

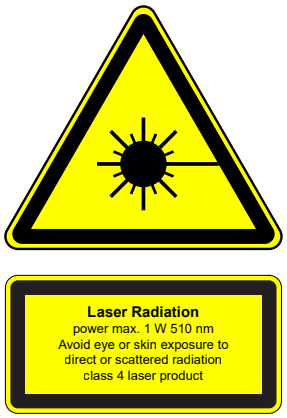

The operators of the diode laser module have to follow the safety precautions found in IEC 60825-1 “Safety of laser products Part 1: Equipment classification, requirements and user’s guide” when connected to the controller.

a.) The laser should only be operated in a supervised laser area

b.) Special care should be taken to avoid unintentional reflections from mirrors

c.) Where possible the laser beam should terminate on a material which scatters the light diffusely after the beam has passed along its intended path. The colour and reflection properties of the material should enable the beam to be diffused, so keeping the hazards due to reflection as low as possible.

d.) Eye protection is necessary if there is a possibility of either direct or reflected radiation entering the eye or diffuse reflections can be seen which do not fulfil the conditions in c.).

e.) The entrances to supervised laser areas should be identified with the laser warning symbol